KONSTAN
JURNAL FISIKA DAN PENDIDIKAN FISIKA
Volume 11, Number 1, June 2026
E-ISSN : 2460-9129 dan P-ISSN : 2460-9110
http://jurnalkonstan.ac.id/index.php/jurnal

Fabrication and Characterization of Eggshell-Derived Nano-CaO Thin Films as Anti-Reflective Coatings: Morphological and Optical Properties

Eka Rahmawati[1,*)], Faridatun Sholehah[2]

[1)]*Physics Education Study Program, Faculty of Education, Nggusuwaru University*
[2)] *Chemistry Education Study Program, Faculty of Education, Nggusuwaru University*

* E-mail correspondence: rahmawatieka89@gmail.com

Article Info:

Sent:
June 22, 2026

Revision:
July 05, 2026

Accepted:
July 06, 2026

Keywords:

Calcium Oxide (CaO), Eggshell Waste, Optical Transmittance, Photovoltaic Glass, Spin Coating, Thin Film

Abstract

Light reflection from glass surfaces reduces the amount of solar radiation transmitted into photovoltaic devices, making transparent thin-film coatings an important approach for improving optical transmission. This study investigated the preparation of calcium oxide (CaO) thin films derived from waste chicken eggshells through a simple and sustainable synthesis route. Eggshell powders were calcined at temperatures ranging from 800 to 1100°C, and the resulting CaO was deposited onto glass substrates by spin coating using five precursor concentrations, followed by post-annealing at 300°C. FTIR and XRD analyses confirmed the gradual decomposition of $CaCO_3$ into crystalline CaO with increasing calcination temperature. The sample calcined at 1100°C exhibited higher crystallinity (80.86%) and a larger crystallite size (19.24 nm) than that calcined at 1000°C. SEM observations indicated that post-annealing reduced the film thickness and produced a more uniform surface morphology. UV–Vis measurements showed that the 0,05 M precursor concentration and has the average thickness of 18,92 nm yielded the highest optical transmittance. The thin film prepared from CaO calcined at 1100°C and post-annealed at 300°C achieved a maximum transmittance of approximately 88% in the visible region (400–900 nm), which was higher than that of the uncoated glass substrate (85%). These results indicate that thermal treatment and precursor concentration significantly influence the structural and optical properties of eggshell-derived CaO thin films, highlighting their potential as transparent coating materials for photovoltaic glass.

INTRODUCTION

One important factor in achieving highly efficient solar cells is the decrease of reflectance. Various antireflection coating techniques are typically applied to the solar cells' upper surface in order to accomplish this. High levels of light transmittance are produced via antireflective (AR) coatings, which reduce the reflection of light shining on them. Any surface where a minimal amount of light loss is needed can have one of these optical coatings applied. To increase the efficiency of solar energy systems, such as photovoltaic and solar thermal devices, it is crucial to do research on attaining a high transmission of light through glass [1,2,3]. These approaches can be separated into three categories: electrochemical etching, sputtering deposition, and thermal oxidation. Several methods for creating anti-reflection coatings include chemical vapor deposition, aerosol pyrolysis sputtering, laser ablation, dip coating, and sol-gel spin coating [4]. In the majority of significant optics applications, reducing optical reflection at the layer interface is a critical difficulty. A single layer coating with a quarter-

wavelength optical thickness and refractive index n = √n1n2, where n1 and n2 are the ambient and substrate refractive indices, respectively, can be used to decrease optical reflection at a certain wavelength [5]. The sol-gel spin coating method is widely employed due to its cost-effectiveness, ability to produce homogeneous layers, applicability at low temperatures, lack of requirement for a high vacuum chamber, and precise control over layer thickness [6].

Conventionally, anti-reflective coating materials are typically derived from inorganic sources such as SiO_2-TiO_2, SiO_2-ZnO, and SiO_2-MgF_2. However, their fabrication process involves considerable cost. The common materials used as AR coating in the visible range are SiO2 (n_c=1.45), Al2O3 (n_c=1.65), MgF2 (n_c=1.38), SiO (n_c=1.85) and ZnO (n_c=2.0), but, none of these materials has such a low RI value [7,8]. In contrast, the development of anti-reflection materials from organic sources remains relatively limited. An innovative alternative involves utilizing CaO derived from waste eggshells. CaO holds potential as a porous anti-reflective material capable of reducing light reflectance through destructive interference effects. An eggshell itself weighs 5–6 grams, containing 1.4 percent magnesium, 85% to 95% $CaCO_3$, and trace amounts of other elements [9]. CaO is a white crystalline solid that can be synthesized from eggshells, which contain $CaCO_3$ as the primary component [10]. CaO produced from waste materials like eggshells can possess a natural porous structure or be engineered into a nano-textured layer. Textured surfaces can aid in light scattering and enhance absorption through diffusion effects. CaO exhibits high thermal stability, making it suitable for applications involving continuous sunlight exposure. It is also resistant to chemical degradation under normal atmospheric conditions, provided it is protected from moisture (as CaO is hygroscopic and reacts to form $Ca(OH)_2$). Common methods for synthesizing CaO nanoparticles include the sol-gel method [11], co-precipitation method [12], and calcination method [13]. The calcination method is particularly effective for converting $CaCO_3$ to CaO, as it is a straightforward, inexpensive, time-efficient process that does not require expensive equipment. During the calcination of eggshells, a thermal decomposition reaction occurs. For $CaCO_3$, calcination is typically conducted at temperatures ranging between 700°C and 1000°C [14].

Although eggshell-derived CaO has been extensively investigated for catalytic, adsorption, and biomedical applications, its use as a transparent thin-film material for anti-reflective coatings remains largely unexplored. Existing studies mainly focus on the synthesis and characterization of CaO powders, while the influence of calcination temperature, post-annealing treatment, and precursor concentration on the structural evolution and optical transmittance of eggshell-derived CaO thin films has received limited attention. Therefore, this study aims to bridge this gap by systematically investigating the relationship between thermal treatment, film morphology, crystallinity, and optical transmittance of spin-coated CaO thin films for potential photovoltaic glass applications. Unlike previous studies [15] that primarily focused on the synthesis and physicochemical characterization of eggshell-derived CaO powders for potential photovoltaic glass applications, this work demonstrates the fabrication of spin-coated CaO thin films and systematically investigates the combined effects of calcination temperature, precursor concentration, and post-annealing treatment on their structural, morphological, and optical properties. Furthermore, the relationship between crystallinity, film thickness, and optical transmittance is established to identify the optimum processing conditions for transparent coating applications.

In this research, CaO will be fabricated in to a thin film using the spin coating method. Utilizing nanoparticles and modifying them into thin films can significantly influence the properties and characteristics of the material. New antireflection sol-gel coatings have garnered a lot of attention lately, mostly because of their affordable price and potential use in a wide range of commercial applications, including high power lasers, architectural glasses, wind screens, solar thermal collectors, solar cells, and video display panels [15,16,17,18,19,20]. Additionally, spin coating and dip coating are effective methods for creating uniform thin films [21]. Annealing treatment of the film will also be conducted in this research to observe the resulting surface morphology. The morphology of a thin film affects its properties and characteristics, thereby determining its suitability for specific applications. Several film properties influenced by morphology include wettability, protein immobilization, optical properties, viscoelastic sensor properties, and sensor sensing capabilities. Research conducted by [22, 23, 24] produced polystyrene thin films with differing morphologies by

utilizing different solvents to enhance protein immobilization. Similarly, [25] performed surface modifications to achieve different viscoelastic properties on QCM sensors. Furthermore, surface wettability can be controlled using spin and spray coating methods [26].

In this study, the structural and optical properties of the fabricated films were evaluated using FTIR and XRD to confirm chemical transformation, SEM to analyze surface morphology, and UV-Vis spectroscopy to measure transmittance. While direct refractive index measurement are beyond the scope of this work, the combination of these techniques provides a comprehensive understanding of the film's suitability for anti-reflective applications. Despite the growing interest in sustainable materials for optical applications, the use of eggshell-derived nano-CaO as an anti-reflective thin film for solar panel applications remains limited. To the best of our knowledge, there is still a lack of systematic studies investigating the relationship between calcination temperature, precursor concentration, post-annealing treatment, and the resulting optical performance of CaO thin films. Therefore, this study aims to fill this gap by optimizing the fabrication parameters and evaluating their influence on the transmittance properties of CaO-based anti-reflective coatings.

METHODE

Extraction of CaO from Eggshells

Chicken eggshells were thoroughly washed and initially sun-dried, followed by oven drying at 120 °C for 2 hours to remove residual moisture. The dried shells were ground using a mortar, pestle, and blender, and subsequently sieved through a 100-mesh sieve. Approximately 200 g of eggshell powder was calcined in a furnace at temperatures ranging from 800 °C to 1100 °C for 3 hours to produce CaO particles. The resulting powders were stored in an airtight container to minimize moisture exposure. Fourier-transform infrared (FTIR) spectroscopy was employed to analyze the chemical composition. While X-ray diffraction (XRD) analysis was performed to identify the crystalline phases present in the eggshell-derived powders and to evaluate the effect of calcination temperature on the structural properties of the synthesized CaO. In addition, XRD data were used to determine the crystallite size using the Scherrer equation and to estimate the degree of crystallinity through the peak area method. The structural information obtained from XRD was further correlated with the optical properties of the resulting thin films.

Formulation and Fabrication of CaO Thin Films

For thin film fabrication, CaO solutions were prepared with concentrations of 0.010 M, 0.050 M, 0.075 M, 0.100 M, and 0.150 M using deionized (DI) water as the solvent. Polyvinyl alcohol (PVA) and citric acid were added as binding agents to improve film adhesion. Each solution was homogenized using an ultrasonic cleaner for 3 hours. Glass substrates were cleaned using 75% ethanol to remove surface contaminants and ensure uniform coating. The films were deposited using a spin coater at 3000 rpm for 60 seconds to obtain single-layer coatings. The coated substrates were dried at room temperature for 1 hour, followed by heating at 100 °C for 30 minutes to remove residual solvent. Post-annealing was then performed at 300 °C for 3 hours to enhance film structure and morphology. Surface morphology was analyzed using scanning electron microscopy (SEM), while optical properties were evaluated using UV–Vis spectroscopy.

Table 1. Concentration of CaO Solution

CaO solutions (M)	CaO (gr)	PVA (gr)	citric acid (gr)
0,01 (cons 1)	0,028	0,5	0,525
0,05 (cons 2)	0,14	0,5	0,525
0,075 (cons 3)	0,21	0,5	0,525
0,1 (cons 4)	0,28	0,5	0,525
0,15 (cons 5)	0,42	0,5	0,525

Each solution was transferred into separate containers and homogenized using an ultrasonic cleaner for 3 hours. Concurrently, the substrate for thin film growth, a glass slide, was pre-cleaned using 75% alcohol. The glass substrate was then mounted onto the spin coater holder for coating with the CaO solution. The coating process was performed at 3000 rpm as a speed of spin coater for 60 second [20] to get the single layer of CaO thin films. The coated glass substrates were left at room temperature for 1 hour. Once dried, the substrates were heated in an oven at 100°C for 30 minutes to ensure the complete removal of any residual solvent. To maximize crystallization, a mild calcination step was performed on the samples at temperatures 300°C for 3 hours. Finally, the CaO modified into thin films was characterized using Scanning Electron Microscopy (SEM) to examine the surface morphology and the thickness of the layers.

Testing the Anti-Reflective Properties of the Thin Films

The optical properties of the CaO thin films were analyzed using UV-Vis spectroscopy by measuring their reflectance and transmission values.

RESULTS AND DISCUSSION

Eggshell powder was calcined at four different temperatures, namely 800°C, 900°C, 1000°C, and 1100°C, to investigate the thermal decomposition behavior of calcium carbonate and its conversion into calcium oxide. Visual observations revealed significant changes in the appearance of the powders after calcination at figure 1. The samples calcined at 1000°C and 1100°C exhibited a uniform bright white color, whereas those calcined at 800°C and 900°C still contained grayish to blackish residues, with the most pronounced discoloration observed in the sample treated at 800°C. These differences in color suggest variations in the degree of thermal decomposition and phase transformation during the calcination process.

a b c D

Figure 1. Egg Shell powder based on temperature of calcination a) 800 °C, b) 900°C, c) 1000 °C, d) 1100 °C

The formation of a bright white powder at higher calcination temperatures indicates a more complete conversion of calcium carbonate ($CaCO_3$), the primary constituent of eggshells, into calcium oxide (CaO). The thermal decomposition of calcium carbonate occurs according to the reaction:

$$CaO\ (s) + CO2\ (g) \rightarrow CaCO3\ (s)$$

This endothermic reaction generally becomes significant above 800°C and proceeds more completely as the calcination temperature increases (Boynton, 1980; Oates, 1998). The persistence of gray and black residues in the samples calcined at 800°C and 900°C may be attributed to incomplete decomposition of $CaCO_3$ and the presence of residual organic matter originating from the eggshell membrane. Previous studies have reported that biogenic calcium carbonate materials often require temperatures above 900°C to achieve complete decarbonation and produce highly pure CaO [27]

Although the formation of a bright white powder at 1000°C and 1100°C indicates a higher degree of thermal decomposition compared with the samples calcined at 800°C and 900°C, direct evidence of phase transformation cannot be obtained solely from visual observations. Consequently, FTIR characterization was employed to examine the changes in chemical bonding and functional groups resulting from calcination. The FTIR analysis is particularly important for monitoring the reduction

of carbonate-related vibrations and confirming the formation of calcium oxide, which is expected to become more pronounced with increasing calcination temperature. The FTIR analysis was critical for monitoring the thermal decomposition of $CaCO_3$ to CaO. Figure 2 shows the FTIR spectra for samples calcined at different temperatures.

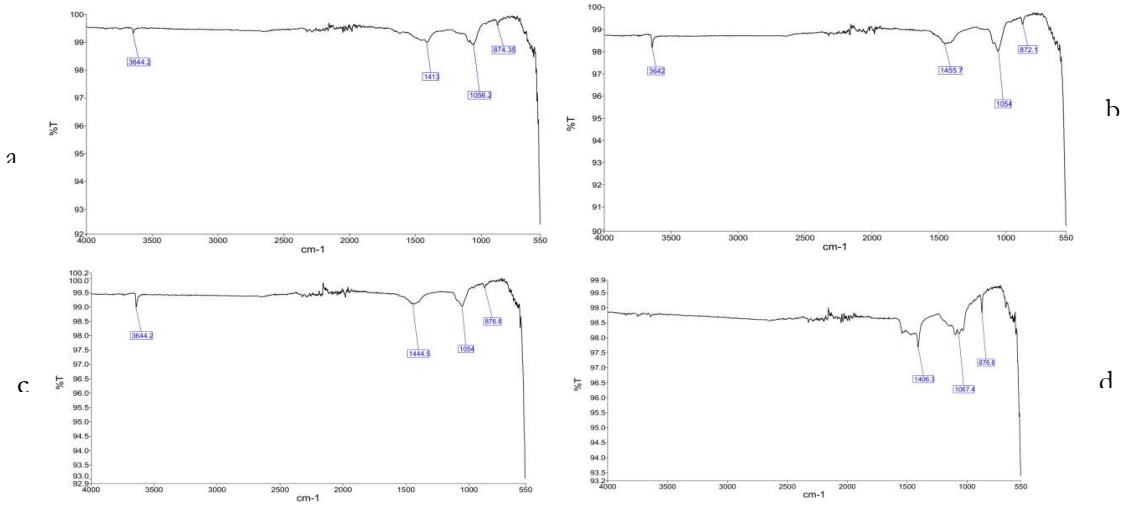

Figure 2. FTIR Characterization for CaO at different calcination temperatures, a) 800^0C, b) 900^0C, c)

The samples calcined at 800°C and 900°C showed strong absorption bands around 874 cm^{-1} and 1413-1455 cm^{-1}, which are characteristic of the asymmetric stretching (ν_3) and out-of-plane bending (ν_2) vibrational modes of the carbonate (CO_3^{2-}) ion, respectively [12]. The presence of a broad band around 3644 cm^{-1} indicates O-H stretching from adsorbed water or $Ca(OH)_2$, formed due to the partial hydration of CaO. As the calcination temperature increased to 1000°C and 1100°C, the intensity of the carbonate peaks (~874 cm^{-1} and ~1450 cm^{-1}) diminished significantly. The spectrum for the 1100°C sample showed the weakest carbonate signals, confirming near-complete decomposition to CaO. The absence of the O-H band in the 1100°C sample suggests higher purity and better stability against hydration post-calcination at the highest temperature [13]. This aligns with the visual observation of pure white powder only at 1000°C and 1100°C. Then in this research we use the 1000°C and 1100°C calcinated CaO to fabricate an antireflecting thin film.

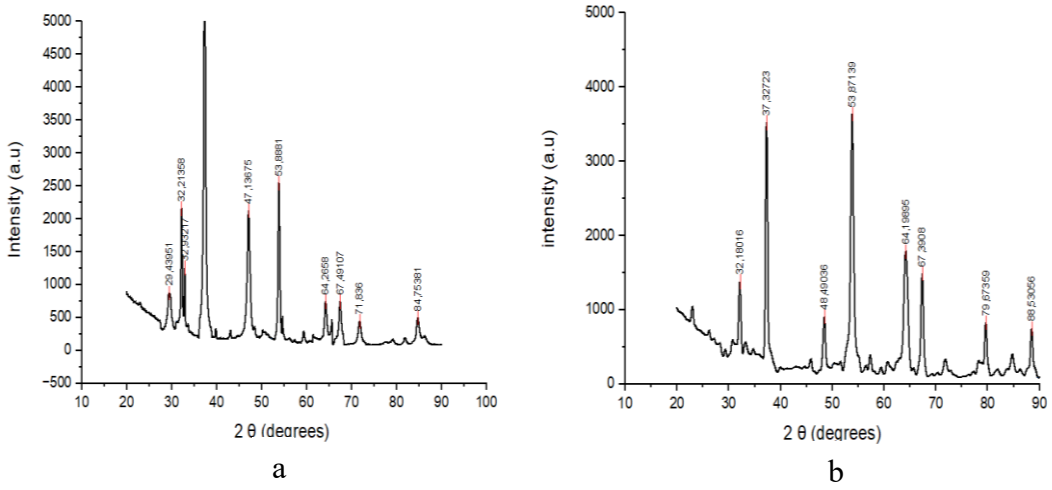

Figure 3. The XRD patterns of CaO calcinated at different temperatures a) 1000 ^{0}C , b) 1100

The phase composition and crystallographic characteristics of the eggshell-derived powders calcined at 1000°C and 1100°C were investigated using X-ray diffraction (XRD), as presented in Figure 3 and table 2 . For the sample calcined at 1100°C, the diffraction peaks observed at 32.18°,

37.33°, 53.87°, 64.20°, 67.39°, 79.67°, and 88.53° closely match the characteristic reflections of crystalline CaO, corresponding to the standard JCPDS data at 32.2°, 37.3°, 53.8°, 64.1°, 67.3°, 79.7°, and 88.5°, respectively. The excellent agreement between the experimental and reference diffraction angles confirms the successful formation of highly crystalline CaO following calcination at 1100°C. The dominant diffraction peaks indicate that calcium oxide became the primary phase after thermal treatment.

Although a weak diffraction peak associated with $CaCO_3$ was still detected at 48.49°, its relatively low intensity suggests that only a small amount of residual carbonate remained in the sample. This residual carbonate may originate from incomplete decomposition of calcium carbonate during calcination or from the recarbonation of CaO upon exposure to atmospheric carbon dioxide during cooling and storage. Similar phenomena have been reported in biogenic CaO materials derived from eggshells and other calcium-rich wastes.

In contrast, the sample calcined at 1000°C exhibited diffraction peaks corresponding to CaO at 32.21°, 37.36°, 53.89°, 64.27°, and 67.49°, confirming that the decomposition of calcium carbonate had already occurred at this temperature. However, additional diffraction peaks assigned to $CaCO_3$ and $Ca(OH)_2$ were also detected. The presence of a $CaCO_3$ peak at 29.44° indicates that a portion of the original calcium carbonate remained undecomposed. Furthermore, diffraction peaks associated with calcium hydroxide were observed at approximately 47.14° and 71.84°, suggesting the hydration of CaO due to moisture absorption from the surrounding environment.

The absence of detectable $Ca(OH)_2$ peaks in the 1100°C sample further suggests improved phase stability. Higher calcination temperatures generally promote grain growth and crystallite development, reducing structural defects and increasing crystallinity. The enhanced crystallinity of the 1100°C sample is evidenced by the sharper and more well-defined diffraction peaks compared with those observed for the 1000°C sample. According to [28] Cullity and Stock (2001), sharper diffraction peaks are typically associated with larger crystallite sizes and improved crystal ordering.

Table 2. Comparison of characteristic XRD diffraction peaks of eggshell-derived powders calcined at different temperatures with JCPDS reference data

Sample	Calcination Temperature	Compound	2 θ (degree)						
JCPDS data	-	CaO	32,2	37,3	53,8	64,1	67,3	79,7	88,5
		CaCO3	29,4	39,4	43,2	47,4	48,5		
		Ca(OH)2	28,6	34,1	47,1	50,8			
Egg Shell	1100	CaO	32,18	37,33	53,87	64,20	67,39	79,67	88,53
		CaCO3					48,49		
		Ca(OH)2							
	1000	CaO	32,21	37,36	53,89	64,27	67,49		
		CaCO3	29,44						
		Ca(OH)2			47,14			71,84	

The crystallite sizes of both structures were estimated using Scherrer's equation and Area Crystallinity Method for observe the crystallinity.

Table 3. The structural Properties of CaO Powders Calcinated at Different Temperature

sample	Calcination Temperature	diameter kisi Kristal (nm)	Crystallinity (%)
Egg Shell	1100	19,244	80,862
	1000	13,361	73,806

The results reveal that increasing the calcination temperature from 1000°C to 1100°C significantly enhanced both the crystallite size and crystallinity of the CaO powders. The crystallite size increased from 13.361 nm to 19.244 nm, while the crystallinity increased from 73.806% to 80.862%. The increase in crystallite size can be attributed to thermally induced crystal growth during calcination. At elevated temperatures, atoms acquire sufficient thermal energy to migrate across grain boundaries, promoting the coalescence of smaller crystallites into larger crystalline domains. This phenomenon reduces the total grain boundary area and lowers the overall free energy of the system, resulting in the formation of larger and more stable crystallites [28]

The higher phase purity and crystallinity obtained at 1100°C are expected to contribute positively to the optical performance of the resulting thin films. The reduction of secondary phases such as $CaCO_3$ and $Ca(OH)_2$ minimizes structural heterogeneity and potential light-scattering centers, thereby enhancing optical transparency and transmittance. This observation is consistent with the UV–Vis results, where the thin films prepared from powders calcined at 1100°C exhibited superior optical transmittance compared with those prepared from powders calcined at 1000°C.

The XRD results support this interpretation. The sample calcined at 1000°C still exhibited diffraction peaks corresponding to residual $CaCO_3$ and $Ca(OH)_2$ phases, indicating incomplete decomposition and secondary phase formation. In contrast, the sample calcined at 1100°C showed predominantly CaO diffraction peaks with only minor traces of carbonate impurities. The reduction of secondary phases contributes directly to the increase in crystallinity observed at higher temperatures.

Higher crystallinity is particularly advantageous for optical coating applications because crystalline materials generally possess fewer structural defects, dislocations, and amorphous regions that can scatter incident light. Defects and phase impurities often act as optical scattering centers, reducing transparency and optical performance. Therefore, the improved crystallinity of the 1100°C sample is expected to enhance the optical transmittance of the resulting thin films. The higher crystallinity and larger crystallite size achieved at 1100°C are expected to positively influence the optical behavior of the deposited CaO thin films. A more crystalline structure generally exhibits lower defect density and reduced optical scattering, which can improve light transmission through the coating. This assumption is supported by the UV–Vis results, where the post-annealed films derived from the 1100°C-calcined powder exhibited the highest transmittance among all investigated samples.

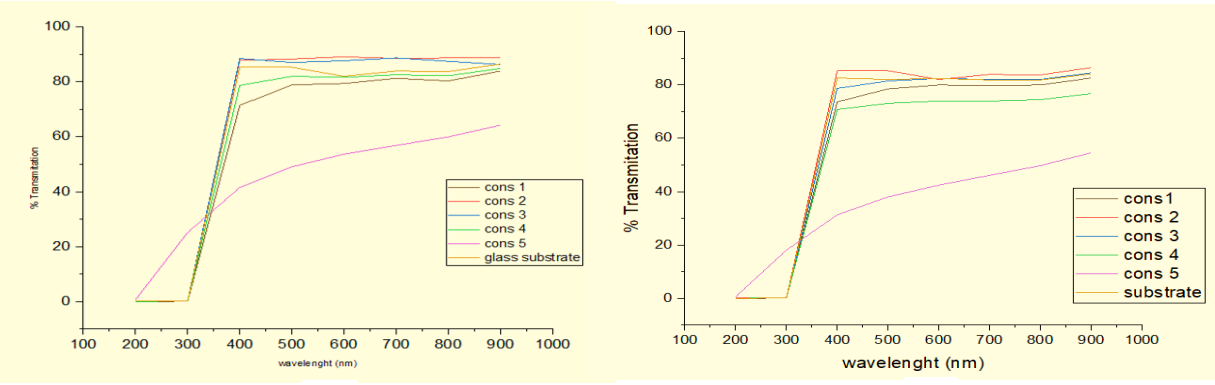

Figure 5. The Optivcal Transmitance Of CaO Thin Films Calcinated at 1100 ^{O}C, a) Without post anneaed, b) post annealed

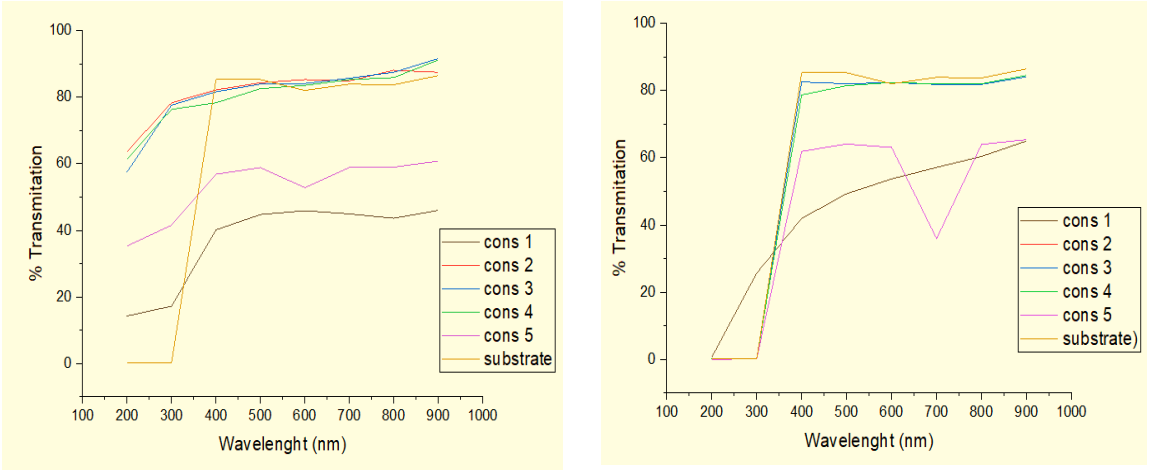

a b

Figure 6. The Optical Transmitance of CaO Thin Film calcinated at 1000 ^{0}C, a) without post annealed, b) post annealed

The optical transmittance spectra of the CaO thin films prepared from waste eggshells at different concentrations and thermal treatments are shown in Figure 5 and figure 6. The results indicate that the optical performance of the films was strongly influenced by both the CaO concentration and the post-annealing treatment. Among all investigated samples, the films prepared from CaO calcined at 1100°C and subsequently post-annealed at 300°C exhibited the highest optical transmittance. In particular, the films with concentrations of 2% and 3% demonstrated superior transmittance throughout the visible and near-infrared regions (400–900 nm).

At low CaO concentrations, the deposited layer may not completely cover the substrate surface, resulting in a limited reduction of optical reflection. In contrast, higher concentrations tend to promote particle agglomeration and produce thicker films, which increase light scattering and consequently reduce optical transmittance. Similar behavior has been reported for oxide-based antireflective coatings, where an optimum coating thickness was found to maximize optical transmission while minimizing scattering effects.

The superior optical performance exhibited by the films calcined at 1100°C can be associated with improved crystallinity and phase purity of CaO. Higher calcination temperatures facilitate the complete decomposition of calcium carbonate into calcium oxide and promote crystal growth, resulting in a more ordered crystal structure with fewer defects [29. Structural defects, grain boundaries, and residual carbonate phases may act as scattering centers for incident light; therefore, their reduction contributes to improved optical transparency [28].

Table 4. Optical performance of eggshell-derived CaO antireflective thin films prepared

Sample	Average Transmittance (400–900 nm) (%)	Maximum Transmittance (%)	Transmittance Enhancement Relative to substrate Bare Glass (%)
		Cons 2	
1000°C, Without Post-Annealing	81,86	84,53	-2,61
1000°C, Post-Annealed at 300°C	85,40	88,10	0,92
1100°C, Without Post-Annealing	85,50	87,90	1,03
1100°C, Post-Annealed at 300°C	88,55	89,13	4,07
Bare Glass	84,48		
		Cons 3	
1000°C, Without Post-Annealing	82,48	84,14	-1,99
1000°C, Post-Annealed at 300°C	84,09	87,50	-0,38
1100°C, Without Post-Annealing	81,86	84,53	-2,61
1100°C, Post-Annealed at 300°C	87,64	88,72	3,16
Bare Glass	84,48		

After annealing, Concentration 2 consistently outperforms Concentration 3, despite Concentration 3's excellent performance and near-optimal performance. This implies that the film produced from Concentration 3 has a slightly higher physical thickness than is optimal. The slightly increased thickness may result in a slight increase in intrinsic absorption or introduce a higher probability for slight inhomogeneities that contribute to weak scattering, but it still encourages strong destructive interference. Although the ideal balance attained by Concentration 2 is not entirely reached, the annealing process still offers considerable advantages by enhancing the film's homogeneity and crystallinity, which accounts for the high transmittance values. With Concentration 4, the performance starts to deteriorate more pronouncedly. There is no doubt that a thicker film results from a higher precursor concentration. When the thickness deviates from the ideal range, the interference condition moves away from the visible spectrum's centre because the $n \times d$ product no longer equals $\lambda/4$ for a given wavelength. Moreover, thicker films deposited from solution frequently experience increased internal stresses as the solvent evaporates, which results in the development of microcracks and a more columnar or porous microstructure from the path of specular transmittance. Although annealing helps the film by repairing some of these flaws, which accounts for the detectable increase in transmittance, it is unable to completely address the underlying problem of excessive thickness and the resulting scattering losses.

The transmittance profile of concentration 5 is essentially different, with consistently low values that are essentially wavelength invariant. This is a well-known sign that high levels of optical loss, rather than interference effects, dominate the optical behaviour. A very thick, structurally flawed film is probably produced by the incredibly high concentration. The film most likely has a high density of voids, cracks, and grain boundaries, all of which serve as powerful scattering canters. Higher intrinsic absorption could also result from the larger material volume. The overwhelming scattering and absorption in this regime completely obscure the subtle constructive and destructive interference patterns. A significant portion of incident light is diffusely scattered due to the lengthy optical path length through this thick, turbid medium. Higher intrinsic absorption could also result from the larger material volume. The overwhelming scattering and absorption in this regime completely obscure the subtle constructive and destructive interference patterns. Although some structural consolidation is achieved through the annealing process, which lowers the defect density and increases transmittance, the film is still too thick and lossy to be a useful anti-reflective layer.

In summary, a shift from an interference-dominated regime to a scattering-dominated regime governs the non-monotonic relationship between precursor concentration and transmittance. The "Goldilocks zone," where the thickness is ideal for utilizing destructive interference, is where Concentrations 2 and 3 are located. After annealing, Concentration 2 among them achieves the most accurate synergy of minimal microstructural defects, appropriate refractive index, and optimal optical thickness. By densifying the material, smoothing surfaces, and annealing out point defects, the annealing process is a crucial enabler that adjusts the film's properties toward their optimal values. This study emphasizes that in order to control the underlying physical optics phenomena and maximize the performance of solution-processed anti-reflective coatings, careful optimization of the deposition chemistry and the post-processing thermal conditions is necessary.

The bare glass substrate showed a baseline transmittance of approximately 82-85% in the visible region (500-800 nm), with the 8% loss attributed to Fresnel reflection. The most significant result was observed for the film from CaO calcined at 1100°C and post-annealed (b). This film achieved a peak transmittance of 87 to 88% at the concentration 0,05 ppm and 0,075 ppm in range wavelength 400 nm-900 nm , while for non-post-annealed films shows 78%-84% amount of transmittance at the same concentration and wavelength, consistently outperforming the bare glass across most of the visible spectrum. Although this presentation under 90%, but this CaO thin films promising to fabricate as an antireflecting films because of amount of transmittance higher then bare glass substrate. This enhancement of ~6% absolute transmittance (or a reduction of over 50% in reflective losses) is a strong indicator of excellent AR performance.

The optical properties of the thin film AR coating are significantly influenced by its microstructure, thickness and refractive index, which all depend on deposition conditions such as precursor concentration and post-deposition heating. The experimental transmittance spectra, in turn,

for various CaO film concentrations prior to and following annealing at 300°C represent a valuable case of the competition among such parameters. The basis of a single layer AR coating is the phenomenon of destructive interference between waves reflected by the air–film and film–substrate interfaces. A distinct pattern emerges when the data is examined concentration by concentration. An extremely thin film is probably produced by concentration 1, which is the most diluted precursor solution. The optical thickness of such a film is insufficient to meet the quarter-wavelength condition across the visible spectrum, even though it may show low absorption. As a result, the destructive interference is not complete, which leads to a lower transmittance than at optimal concentrations due to a higher Fresnel reflection. Additionally, the film might be too porous or discontinuous, which would increase light scattering at the rough interfaces and further lower the direct transmittance. Densification and defect reduction following annealing result in some improvement, but the intrinsic limitation of inadequate thickness keeps it from performing at its best. On the other hand, Concentration 2 exhibits the best results, especially following the annealing procedure. It is assumed that this particular concentration creates a physical thickness that, following the structural changes brought about by annealing, yields an optical thickness for destructive interference that is almost flawless over a wide range of the visible spectrum. According to the morphological analysis, the annealing process at 300°C promotes the densification of the CaO layer, removing micro-porosity and decreasing surface roughness.

SEM analysis provided insights into the surface morphology of the spin-coated films, which directly influences their optical properties. Figure 2 presents SEM micrographs of films fabricated from CaO calcined at 1000°C and 1100°C, with and without post-annealing.

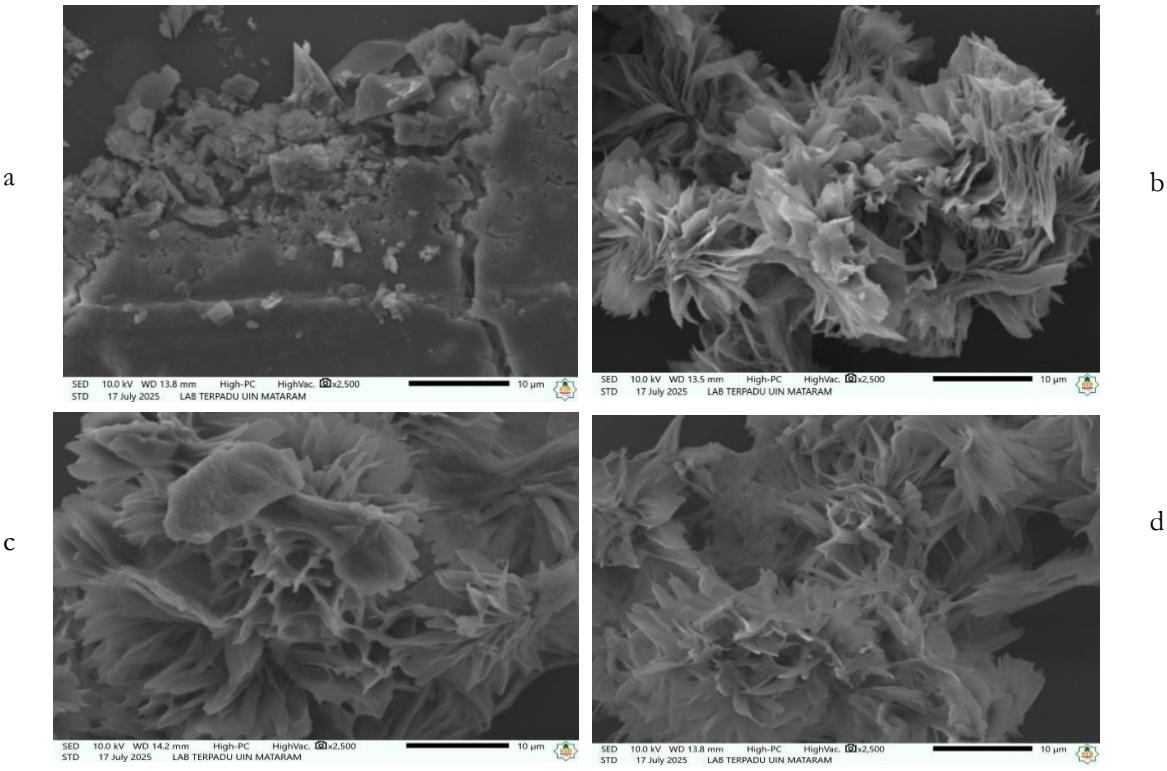

Figure 7. SEM images of CaO thin films: a) CaO-1000°C without annealing, b) CaO-1000°C post-annealing, a) CaO-1100°C without annealing, b) CaO-1100°C post annealing

Films without post-annealing (a) exhibited a relatively dense and granular structure with some agglomeration. The surface appeared less uniform, which could lead to increased light scattering. In contrast, films that underwent post-annealing at 300°C (b) displayed a remarkable transformation. The morphology became more homogeneous, with the development of a nano-porous films. This porosity arises from the burnout of the organic binders (PVA, citric acid) and the subsequent sintering of CaO nanoparticles. This study highlights the significant role of particle size in tailoring the structural and optical properties of CaO thin films for practical optical device applications [29]. A porous structure necessary for reaching a low RI can be produced using the sol-gel process, one of

several coating procedures, and the distribution of pores within the structure can be controlled [30]. This nano-porous structure is highly desirable for AR coatings, as the pores (filled with air, n=1) lower the effective refractive index (n eff) of the film according to the effective medium theory. The annealed layer in figure (b) shows the smaller porous than films at figure (a). Larger pores lead to decreased optical transmittance but an increase in reflectance, absorbance, and refractive index due to enhanced light scattering and light trapping within the films [31]. A lower n_eff is crucial for better impedance matching between air and the glass substrate, thereby reducing reflection. Annealing temperature has a significant influence on the structural, morphological, and optical properties. Higher annealing temperatures improve crystallinity, enlarge grain and crystallite size, and increase surface roughness [32]. The film annealed at 300°C demonstrated an optimal cobination of high crystallinity and God optical transmittance, making it particularly suitable for applications such as anti-reflection coatings, dye-sensitized solar cells, and various optoelectronic devices. The ability to tune these properties through annealing makes nanostructured CaO a versatile material for advanced technological applications. In conclusion, the study demonstrates that the annealing temperature significantly influences the properties CaO thin films. The high transparency and tunable wide band gap make these films promising materials for applications in solar cells, gas sensors, and transparent electrodes for display panels [33]

From the figure 7, it shows that the morphology of films seems like the sharp tipped nanoflower structures. The sharp tips create a smoother and more progressive transition from air to the solid material. The sharp-tipped structure ensures that the solid volume fraction (fill factor) decreases in an almost linear manner from the base to the peak. This more perfect gradient results in lower reflection, especially for shorter wavelengths (blue/UV light), which are highly sensitive to gradient imperfections. This directly enhances transmittance across the entire spectrum, with the most significant improvement occurring in the near-UV to blue region. The superior performance of the (b) film can be attributed to two synergistic factors, high purity CaO FTIR confirmed that 1100°C calcination yielded the purest CaO, minimizing light absorption by residual carbonates. Optimal Nano-Porosity as a SEM showed that post-annealing created an ideal nano-porous structure in the (b) films. This porosity effectively reduces the n_eff. Furthermore, the post-annealing process likely optimizes the film's thickness [23], bringing it closer to the quarter- wavelength (λ/4) condition for destructive interference at the central visible wavelength

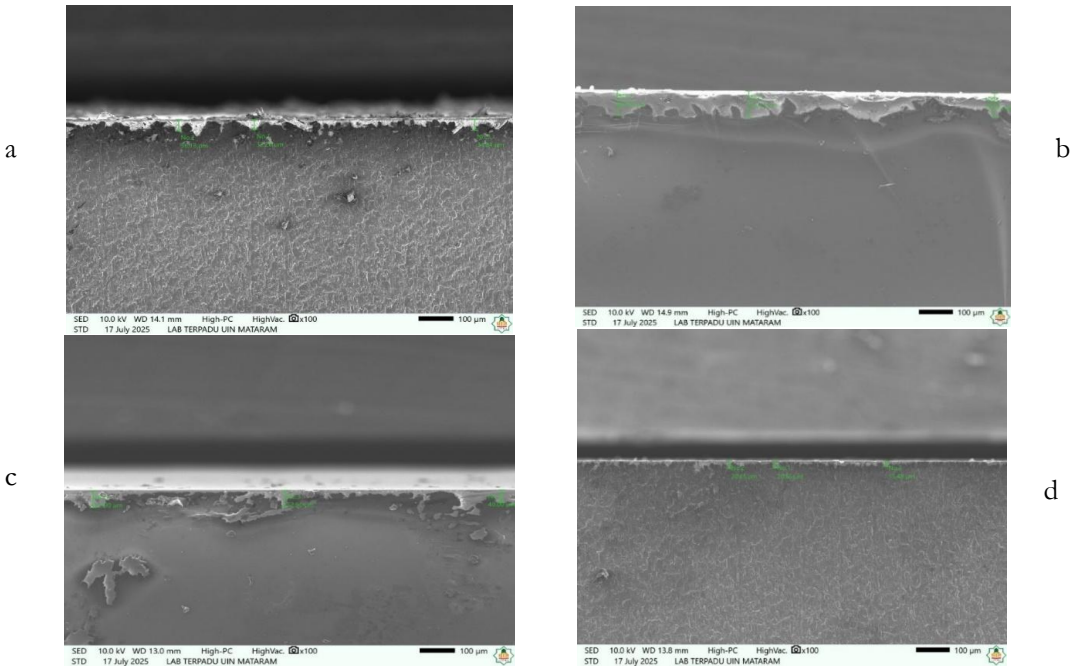

Figure 8. Cross-sectional SEM images illustrating the thickness of CaO thin films prepared under different calcination temperatures and post-annealing conditions, (a) calcined at 1000°C without post-annealing, (b) calcined at 1000°C with post-annealing at 300°C, (c) calcined at 1100°C without post-annealing, and (d) calcined at 1100°C with post-annealing at 300°C.

Table 5. Comparison of the thickness of CaO thin films prepared at different calcination temperatures with and without post-annealing treatment.

Calcination Temperature (°C)	Thickness of CaO Thin Films					
	Without Annealing (μm)			With Post-Annealing at 300°C (μm)		
	1	2	3	1	2	3
1000	85,16	80,04	74,71	32,26	36,13	34,84
1100	52,9	40	52,9	20,65	20,65	15,48

Furthermore, post-annealing treatment at 300°C significantly enhanced the optical transmittance of the films based on data tabel 2. SEM analysis revealed a considerable reduction in film thickness after annealing, indicating densification of the coating structure. Thermal annealing promotes solvent evaporation, particle rearrangement, and pore shrinkage, leading to a denser and more homogeneous microstructure [34] (Ohring, 2002). Such structural refinement reduces light scattering and allows a greater fraction of incident light to pass through the coating. According to thin-film optical theory, antireflective performance is strongly dependent on film thickness and uniformity, where excessively thin films fail to effectively modify the optical interface, while excessively thick films increase optical scattering losses [35] (Macleod, 2010).

It is important to note that film thickness and refractive index are critical parameters governing anti-reflective performance. In this study, these parameters were not directly measured, which represents a limitation in fully validating the quarter-wavelength condition. Nevertheless, the observed trends in transmittance as a function of precursor concentration and annealing treatment provide indirect evidence of thickness and refractive index variation. The existence of an optimal concentration suggests that the film thickness approaches a condition favorable for destructive interference. Future work should include direct measurements refractive index (e.g., ellipsometry or Swanepoel method) to provide a more comprehensive optical analysis. A limitation of this study is the use of a single-layer coating. Multilayer coatings, such as a double- layer with graded refractive indices, could potentially yield even higher transmittance gains [36]. High-quality multilayer antireflective coatings via a sol-gel process that balance optical performance and surface stability. The study highlights the importance of multilayer design in optical coatings for maximizing transmittance across a broad visible spectrum [37]

Furthermore, long-term stability tests under real-world environmental conditions (humidity, UV exposure, thermal cycling) are necessary to assess the coating's durability, given CaO's hygroscopic nature. The implications of this research are twofold. Scientifically, it demonstrates a novel pathway for designing sustainable optical materials from waste streams. Practically, it presents a cost-effective and eco-friendly method to enhance solar panel efficiency, contributing to both waste management and the advancement of renewable energy technology.

CONCLUSION

This study successfully demonstrated the fabrication and optimization of nano-CaO thin films derived from chicken eggshell waste for application as an anti-reflective coating. Calcination temperature critically determines the purity of CaO, with 1100°C identified as the optimal condition for complete decomposition of $CaCO_3$. A post-annealing treatment at 300°C after spin coating is essential for developing a nano-porous morphology in the thin film. The synergistic effect of high-purity CaO (from 1100°C calcination) and an optimal nano-porous structure (from post-annealing) resulted in a thin film with a peak optical transmittance of 88,5%, significantly surpassing the performance of uncoated glass. The research conclusively proves that eggshell-derived nano-CaO is a highly promising and high-performance material for anti-reflective coatings in solar panel

applications. For future work, it is recommended to explore multilayer designs, conduct rigorous environmental stability tests, and perform in-situ efficiency measurements on functional solar cells.

ACKNOWLEDGEMENT

The authors gratefully acknowledge the financial support provided by the Indonesian Ministry of Education, Culture, Research, and Technology through the "Penelitian Dasar". We also extend our gratitude to the Laboratory of UIN Mataram for providing access to their characterization facilities.

REFERENCE

[1] X. Huang, Y. Yuan, S. Liu, L. Zhang, and R. Hong, "Preparation of hydrophobic broadband antireflective SiO_2 coating on flexible poly(methyl methacrylate) substrates," *Colloids Surf. A Physicochem. Eng. Asp.*, vol. 538, pp. 519–525, Feb. 2018, doi: https://doi.org/10.1016/j.colsurfa.2017.11.027

[2] C. Agustín-Sáenz, M. Machado, and A. Tercjak, "Antireflective mesoporous silica coatings by optimization of water content in acid-catalyzed sol-gel method for application in glass covers of concentrated photovoltaic modules," *J. Colloid Interface Sci.*, vol. 534, pp. 370–380, Jan. 2019, doi: https://doi.org/10.1016/j.jcis.2018.09.043

[3] M. S. Mozumder, A.-H. I. Mourad, H. Pervez, and R. Surkatti, "Recent developments in multifunctional coatings for solar panel applications: A review," *Sol. Energy Mater. Sol. Cells*, vol. 189, pp. 75–102, Jan. 2019, doi: https://doi.org/10.1016/j.solmat.2018.09.015

[4] Z. Liang, W. Li, B. Dong, Y. Sun, H. Tang, L. Zhao, and S. Wang, "Double-function SiO_2-DMS coating with antireflection and superhydrophobic surface," *Chem. Phys. Lett.*, vol. 716, pp. 211–214, Jan. 2019. Doi: https://doi.org/10.1016/j.cplett.2018.12.030

[5] W. H. Southwell, "Coating design using very thin high- and low-index layers," *Appl. Opt.*, vol. 24, no. 4, pp. 457–460, Feb. 1985, doi: https://doi.org/10.1364/AO.24.000457

[6] W. Slamet, "Teknologi sol-gel pada pembuatan nano kristalin metal oksida untuk aplikasi sensor gas," presented at the *Seminar Rekayasa Kimia dan Proses*, Semarang, Indonesia, 2010.

[7] B. G. Priyadarshini and A. K. Sharma, "Design of multi-layer anti-reflection coating for terrestrial solar panel glass," *Bull. Mater. Sci.*, vol. 39, no. 3, pp. 683–689, May 2016, doi: https://link.springer.com/article/10.1007/s12034-016-1195-x

[8] İ. G. Kavaklı and K. Kantarlı, "Single and double-layer antireflection coatings on silicon," *Turk. J. Phys.*, vol. 26, pp. 349–354, 2002.

[9] O. Awogbemi, F. Inambao, and E. I. Onuh, "Modification and characterization of chicken eggshell for possible catalytic applications," *Heliyon*, vol. 6, no. 10, Art. no. e05283, Oct. 2020, doi: https://doi.org/10.1016/j.heliyon.2020.e05283

[10] A. Y. Nuryantini, C. D. D. Sundari, Halimahtussa'diah, and B. W. Nuryadin, "Synthesis and characterization of calcium oxide nanoparticles from duck eggshells using ball milling methods," *J. Kim. Valensi*, vol. 5, no. 2, pp. 231–235, Nov. 2019.

[11] L. Habte, N. Shiferaw, D. Mulatu, T. Thenepalli, R. Chilakala, and J. W. Ahn, "Synthesis of nano-calcium oxide from waste eggshell by sol-gel method," *Sustainability*, vol. 11, no. 11, Art. no. 3196, Jun. 2019, doi: https://doi.org/10.3390/su11113196

[12] Y. M. Alobaidi, M. M. Ali, and A. M. Mohammed, "Synthesis of calcium oxide nanoparticles from waste eggshell by thermal decomposition and their applications," *Jordan J. Biol. Sci.*, vol. 15, no. 2, pp. 269–274, Jun. 2022.

[13] D. K. Dewi, V. M. Putri, V. Febriyanti, and C. S. Yudha, "Calcination of various eggshell wastes into CaO heterogeneous catalysts," *Equilibrium J. Chem. Eng.*, vol. 7, no. 1, pp. 87–92, Jul. 2023. Doi: https://dx.doi.org/10.20961/equilibrium.v7i1.74484

[14] S. Arita, S. A. Adelia, and D. P. Sari, "Pembuatan katalis heterogen dari cangkang kerang darah (*Anadara granosa*) dan diaplikasikan pada reaksi transesterifikasi dari crude palm oil," *J. Tek. Kim.*, vol. 20, no. 3, 2014.

[15] I. H. Hassan, S. U. Muhammad, and O. O. Ige, "Modification and characterization of chicken eggshell for possible photovoltaic glass applications," *Lafia J. Sci. Ind. Res.*, vol. 3, no. 2, pp. 86–94, Jun. 2025, doi: 10.62050/ljsir2025.v3n2.589.

[16] R. Prado, G. Beobide, A. Marcaide, J. Goikoetxea, and A. Aranzabe, "Development of multifunctional sol-gel coatings: Anti-reflection coatings with enhanced self-cleaning capacity," *Sol. Energy Mater. Sol. Cells*, vol. 94, no. 6, pp. 1081–1088, Jun. 2010. https://doi.org/10.1016/j.solmat.2010.02.031

[17] L. Gao and J. He, "A facile dip-coating approach based on three silica sols to fabrication of broadband antireflective superhydrophobic coatings," *J. Colloid Interface Sci.*, vol. 400, pp. 24–30, Jun. 2013.DOI: https://doi.org/10.1016/j.jcis.2013.03.013

[18] B. G. Kum, Y. C. Park, Y. J. Chang, J. Y. Jeon, and H. M. Jang, "Single-layered porous silica films on polyethylene terephthalate substrates for antireflection coatings," *Thin Solid Films*, vol. 519, no. 12, pp. 3778–3781, Apr. 2011. Doi: https://doi.org/10.1016/j.tsf.2010.12.163

[19] Y. Du, H. He, Y. Jin, F. Kong, H. Guan, and Z. Fan, "Graded porous glasses for antireflective applications formed by chemical treatment," *Appl. Surf. Sci.*, vol. 258, no. 17, pp. 6431–6435, Jun. 2012. Doi: https://doi.org/10.1016/j.apsusc.2012.03.055

[20] O. Kesmez, H. E. C. Amarillo, E. Burunkaya, and E. Arpac, "Preparation of antireflective SiO_2 nanometric films," *Ceram. Int.*, vol. 36, no. 2, pp. 391–394, Mar. 2010. http://doi.org/10.1016/j.ceramint.2009.07.030

[21] B. T. Liu and W. D. Yeh, "Antireflective surface fabricated from colloidal silica nanoparticles," *Colloids Surf. A Physicochem. Eng. Asp.*, vol. 356, no. 1–3, pp. 145–149, Mar. 2010. Doi : https://doi.org/10.1016/j.colsurfa.2010.01.003

[22] Š. Kment, I. Gregora, H. Kmentová, P. Novotná, Z. Hubička, J. Krýsa, *et al.*, "Raman spectroscopy of dip-coated and spin-coated sol–gel TiO_2 thin films on different types of glass substrate," *J. Sol-Gel Sci. Technol.*, vol. 63, no. 3, pp. 294–306, Sep. 2012, doi: https://link.springer.com/article/10.1007/s10971-012-2787-6

[23] Masruroh, D. J. D. H. Djoko, D. L. A. Didik, E. Rahmawati, M. Pagaga, and S. P. Sakti, "Solvent effect on morphology of polystyrene coating and their role to improvement for biomolecule immobilization in application of QCM based biosensor," in *Appl. Mech. Mater.*, vol. 530, Zurich, Switzerland: Trans Tech Publications, 2014, pp. 54–57. Doi: https://doi.org/10.4028/www.scientific.net/AMM.530-531.54

[24] S. P. Sakti, E. Rahmawati, and F. Robiandi, "Solvent effect on polystyrene surface roughness on top of QCM sensor," in *AIP Conf. Proc.*, vol. 1719, Melville, NY, USA: AIP Publishing, 2016, Art. no. 030017. Doi : https://doi.org/10.1063/1.4943712

[25] E. Rahmawati, *et al.*, "Effect of xylene and tetrahydrofuran solvent type on polystyrene layer thickness with spin coating method," *Nat. B*, vol. 2, no. 4, pp. 349–354, 2014. Doi : https://doi.org/10.21776/ub.natural-b.2014.002.04.9

[26] S. Rahayu, M. Masruroh, D. J. D. H. Santjojo, E. Rahmawati, D. L. A. Didik, F. Robiandi, and S. P. Sakti, "Effects of polystyrene solvent difference on morphology of polystyrene layers and viscoelastic properties of QCM biosensors," *Nat. B*, vol. 2, no. 4, pp. 343–348, 2014. Doi: https://doi.org/10.21776/ub.natural-b.2014.002.04.8

[27] E. Rahmawati and S. Agustina, "Rekayasa permukaan lapisan tipis kitosan sebagai dasar pengembangan teknologi self-cleaning," *Gravity Edu: J. Pembelajaran dan Pengajaran Fis.*, vol. 1, no. 2, pp. 16–19, 2018. Doi : https://doi.org/10.33627/ge.v1i.2.95

[28] E. M. Rivera, M. Araiza, W. Brostow, V. M. Castaño, J. Díaz-Estrada, R. Hernández, and J. R. Rodríguez, "Synthesis of hydroxyapatite from eggshells," *Mater. Lett.*, vol. 41, no. 3, pp. 128–134, Nov. 1999. Doi : https://doi.org/10.1016/S0167-577X(99)00118-4

[29] B. D. Cullity and R. J. Smoluchowski, "Elements of X-ray diffraction," *Phys. Today*, vol. 10, no. 3, pp. 50–50, Mar. 1957.

[30] R. S. Boynton, *Chemistry and Technology of Lime and Limestone*. New York, NY, USA: John Wiley & Sons, 1980.

[31] P. N. Nirmala and G. Suresh, "Influence of the particle size on the optical properties of CaO thin film," *Int. J. Recent Sci. Res.*, vol. 4, no. 9, pp. 1320–1322, Sep. 2013. Doi : https://api.semanticscholar.org/CorpusID:216147317

[32] C. Atkinson, C. L. Sansom, H. J. Almond, and C. P. Shaw, "Coatings for concentrating solar systems—A review," *Renew. Sustain. Energy Rev.*, vol. 45, pp. 113–122, May 2015, doi: https://doi.org/10.1016/j.rser.2015.01.015

[33] D. L. Domtau, J. Simiyu, E. O. Ayieta, G. M. Aslimwe, and J. M. Mwabora, "Influence of pore size on the optical and electrical properties of screen printed TiO_2 thin films," *Adv. Mater. Sci. Eng.*, vol. 2016, Art. no. 7515802, pp. 1–8, 2016, doi: https://doi.org/10.1155/2016/7515802

[34] S. Sönmezoglu, G. Çankaya, and N. Serin, "Influence of annealing temperature on structural, morphological and optical properties of nanostructured TiO_2 thin films," *Mater. Technol.*, vol. 27, no. 3, pp. 251–256, 2012, doi: https://doi.org/10.3390/cryst10060454

[35] M. Ohring, *Materials Science of Thin Films: Deposition and Structure*, 2nd ed. San Diego, CA, USA: Academic Press, 2002.

[36] H. A. Macleod, *Thin-Film Optical Filters*, 4th ed. Boca Raton, FL, USA: CRC Press, 2010.

[37] P. N. Nirmala, G. Suresh, and K. Karunakaramoorthy, "Influence of annealing temperature on optical properties of CaO thin films," *Int. J. Recent Sci. Res.*, vol. 4, no. 4, pp. 425–427, Apr. 2013.

[38] N. Lari, S. Ahangarani, and A. Shanaghi, "Effect of different TiO_2–SiO_2 multilayer coatings applied by sol-gel method on antireflective property," *J. Mater. Eng. Perform.*, vol. 24, no. 7, pp. 2645–2652, Jul. 2015, doi: https://link.springer.com/article/10.1007/s11665-015-1547-5